Synthesis and Photophysical Properties of Ternary I–III–VI AgInS2 Nanocrystals: Intrinsic versus Surface States

ARTICLE *in* THE JOURNAL OF PHYSICAL CHEMISTRY C · APRIL 2011

Impact Factor: 4.77 · DOI: 10.1021/jp2011183

4 AUTHORS, INCLUDING:

Baodong Mao
University of Nebraska at Lincoln
37 PUBLICATIONS **758** CITATIONS

SEE PROFILE

Chi-Hung Chuang
University of Colorado at Boulder
20 PUBLICATIONS **471** CITATIONS

SEE PROFILE

Clemens Burda
Case Western Reserve University
172 PUBLICATIONS **14,613** CITATIONS

SEE PROFILE

THE JOURNAL OF PHYSICAL CHEMISTRY C

ARTICLE

pubs.acs.org/JPCC

Synthesis and Photophysical Properties of Ternary I−III−VI $AgInS_2$ Nanocrystals: Intrinsic versus Surface States

Baodong Mao, Chi-Hung Chuang, Junwei Wang, and Clemens Burda*

Center for Chemical Dynamics and Nanomaterials Research, Department of Chemistry, Case Western Reserve University, 10900 Euclid Avenue, Cleveland, Ohio 44106, United States

Supporting Information

ABSTRACT: Ternary I−III−VI $AgInS_2$ (AIS) semiconductor nanocrystals (NCs) with strong photoluminescence (PL) were synthesized using a one-pot reaction at low temperature. UV−vis absorption and PL spectra red shifted as the AIS NCs grew. Both steady-state and time-resolved PL spectroscopies were used to investigate the influence of surface and intrinsic trap states on the PL behaviors of the prepared AIS NCs. PL lifetimes at different wavelengths in the full spectrum range were measured using a streak camera for each sample toward a systematic kinetic study. We found PL lifetime components that were short-lived from surface states and long-lived from intrinsic states. Surface trap emissions were wavelength- and size-dependent. Besides these PL studies, we report the first measurements using femtosecond transient absorption spectroscopy to investigate the exciton dynamics of the AIS NCs. Because of the abundant intrinsic trap states, these ternary AIS NCs have long-lived excitons, which may provide potential applications in photocatalysis and photovoltaics.

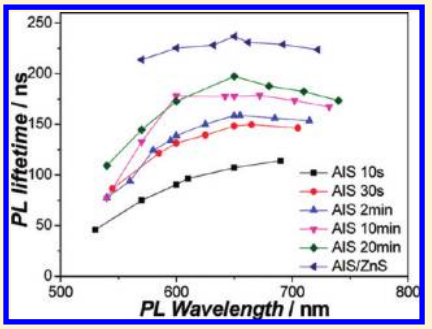

1. INTRODUCTION

Ternary I−III−VI semiconductors exhibit a wide range of applications in light-emitting diodes and lasers, solar cells, and photocatalysis.[1−3] These materials, such as $CuInS_2$ (CIS) and $AgInS_2$ (AIS), are usually direct-band-gap semiconductors with suitable band gaps and high extinction coefficients in the visible-to-near-infrared region. Because of their outstanding luminescent properties, these compounds also attract lots of interest as an alternative for the more toxic cadmium-containing quantum dots (QDs).[4,5]

The I−III−VI quantum dots are of great interest for fundamental studies and technical applications, such as biomedical labeling, light-emitting diodes, solar cells, and sensors, among which, printable solar cells[6,7] and bioimaging[8−10] have attracted attention in recent years. The characteristics of I−III−VI QDs in biosystems include long photoluminescence (PL) lifetimes and low toxicity, both of which are crucial for related applications.[8,11]

Among the I−III−VI semiconductors, AIS nanocrystals (NCs) are attracting more and more attention in the past few years. Several methods have been reported for the synthesis of ternary AIS NCs with adjustable sizes based on thermolysis of various metal−sulfur complexes or direct reaction of metal cations and sulfur with suitable capping reagents.[12−18] The metal cations are usually coordinated with amines or dodecanethiol to form metal complex precursors to ensure controllable particle growth.[12,15,16,18] The sulfur source could be elemental sulfur, thiols, dithiocarbamates, or carbon disulfide that can be dissolved in organic solvents.[12,14,15,17,18] Metal thiolates or dithiocarbamates were also used as single-source precursors for both metal cations and sulfur.[14,17,18] Xie et al. demonstrated several important factors to obtain high-quality I−III−VI NCs, such as coordination of the metal ions by thiols and keeping the precursors at a low concentration.[16] In the case of silver-involved compounds, the reaction can proceed at relatively low temperature because of the fast reaction between Ag and the chalcogens, which is good because low-cost ordinary solvents, such as toluene, can now be used instead of the relatively expensive high-boiling-point solvents.

Most of the recent research on AIS NCs has been focused on the luminescence properties. Although AIS is one of the least-studied I−III−VI semiconductors, the interest on the optical properties of it can date back to the 1970s.[19] Redjai et al studied the donor−acceptor pair transitions in bulk $AgInS_2$ by analyzing time-resolved (TR) spectra and the thermal quenching curve of the emission.[20] The role of the different kinds of defects, such as vacancies and interstitial atoms in the donor−acceptor pair transition, were studied in detail in both bulk and thin-film AIS with ever growing interest.[21−23] In recent work on AIS NCs, wide PL peaks and relatively large Stokes shifts were always observed, which could be assigned to the characteristics of donor−acceptor pair transitions.[16−18,24] Several works were also performed for the study of PL enhancement or quenching of AIS/ZnS NCs in different environments.[25−27] In Ogawa's[18] and Hamanaka's[24] recent works, time-resolved spectroscopy studies were conducted toward the exploration of the PL mechanism of the AIS NCs. Two important conclusions were drawn: the PL

Received: February 2, 2011
Revised: April 3, 2011
Published: April 20, 2011

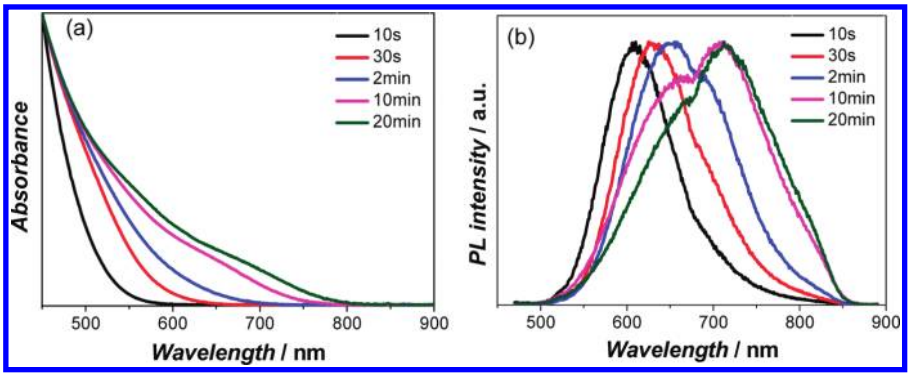

Figure 1. (a) UV−vis absorption and (b) PL spectra of the $AgInS_2$ NCs synthesized at 90 °C for different reaction times shown in the legend. The red shift in both spectra is observed as the reaction time increases due to the particle growth. The detailed discussion of asymmetric PL peaks is addressed in the text.

spectra were excitation intensity-dependent, and the PL lifetime were wavelength-dependent. A time-resolved PL (TRPL) study was also carried out on other I−III−VI NCs ($CuInS_2$ and $CuInS_2$/ZnS) with similar techniques and could be consulted for the study of AIS.[8,28−31] However, due to the lack of systematic time-resolved spectroscopic studies, there is still no clear demonstration of the PL mechanism for these ternary NCs, especially for the difference from bulk materials. In addition, other aspects need to be considered, such as surface defects, due to the high surface-to-volume ratio in small NCs.

In the present work, ternary I−III−VI $AgInS_2$ NCs with tunable sizes and optical properties were synthesized by a one-pot reaction in toluene at low temperature. Time-resolved PL is used to investigate the PL behaviors of the NPs of different sizes. PL lifetimes at different wavelengths in the full spectrum range were also measured for each sample, which show an interesting and systematic wavelength dependence different from a previous report.[18] Femtosecond transient absorption (TA) spectroscopy was used to investigate the excited-state population dynamics of the AIS NCs for the first time. Extremely long-lived excitons were observed and showed almost no decay up to 3 ns in the different-sized AIS NCs. The role of surface and intrinsic defects in the PL process are discussed based on these TR spectra.

2. EXPERIMENTAL SECTION

2.1. Chemicals. Indium acetylacetonate ($In(acac)_3$, 98%, Strem), silver nitrate ($AgNO_3$, 99.5%, Aldrich), sulfur (99.5%, Aldrich), zinc stearate (99.5%, Aldrich), dodecanethiol (DT, 99%, Aldrich), trioctylphosphine (TOP, 90%, Aldrich), oleic acid (OA, 90%, Aldrich), toluene (99.5%, Fischer Scientific), and ethanol (anhydrous, Fischer Scientific) were used as purchased without further purification.

2.2. Synthesis of $AgInS_2$ NCs. The synthesis procedure was derived from Xie's method for CIS and AIS NCs[16] with revisions on solvent and temperature. A 0.5 mmol portion of $AgNO_3$, 0.5 mmol of $In(acac)_3$, 2 mmol of oleic acid, and 20 mL of toluene in a 50 mL flask were heated to 60 °C under an Ar flow and kept for 20 min to exclude oxygen. After that, 5 mmol of DT was injected and the solution was heated to 90 °C. After a clear solution of the metal precursors was obtained, a small amount of TOP (~0.2 mL) was injected, and then 1 mmol of sulfur dissolved in 2.5 mL of toluene was swiftly injected into the system. Aliquots were extracted at different time intervals and injected into an equal amount of cold toluene to get differently sized NCs. After synthesis, the NCs were washed three times with the toluene/ethanol cycle by centrifugation and then dissolved in toluene for storage.

2.3. Synthesis of $AgInS_2$/ZnS NCs. A 0.1 mmol portion of zinc stearate was dispersed into a 3 mL toluene solution of 0.1 mmol of S and 1 mmol of DT by sonification to form the Zn/S/DT dispersion. For the synthesis of AIS/ZnS NCs, the as-synthesized AIS NCs (AIS 2 min, 5 mL) were extracted by a syringe and injected into the toluene solution of Zn/S/DT under stirring. The mixed solution was put into a Teflon-lined stainless steel autoclave and then put into an oven preheated to 210 °C. After staying for 30 min, the autoclave was allowed to cool to room temperature and the AIS/ZnS NCs were cleaned as above. The starting molar ratio of Ag/In/Zn was controlled to 1:1:1.

2.4. Characterizations. UV−vis absorption and PL spectra were recorded using a Varian Cary 50 spectrometer and a Varian Eclipse fluorescence spectrometer with excitation at 450 nm, respectively. Fluorescence quantum yields (QYs) of the NCs were calculated by comparison with a standard dye Rhodanmine B.[32] The size and morphology of the NCs were characterized with a transmission electron microscope (TEM, Philips CM12) at an accelerating voltage of 60 kV. Femtosecond TA measurements were conducted using a Clark MXR 2001 femtosecond laser system that produces 780 nm, 150 fs pulses from a regenerative amplifier.[33−37] A tunable (460−1100 nm) pump pulse from an optical parametric amplifier (OPA, TOPAS, Lightconversion) and a white light continuum (450−800 nm) probe pulse generated in a sapphire crystal are from splitting the laser pulse train. The instrumental time resolution was estimated to be ~150 fs. All TA measurements were conducted in a 2 mm cuvette at room temperature. Time-resolved PL (TRPL) spectra were recorded with a Streak camera (Optronis) with excitation at 470 nm from the OPA.

3. RESULTS

We used steady-state UV−vis absorption and PL spectroscopies to characterize optical properties of the prepared AIS NCs. Figure 1 shows the normalized UV−vis absorption and PL spectra as well as the reaction time in the legend. As the reaction time increases, the absorption and emission continuously moved to lower energy, showing the growing size and reducing confinement effect. The broad absorption (Figure 1a) without a sharp exciton band in our AIS NCs is an indicative feature of ternary compounds.[16−18]

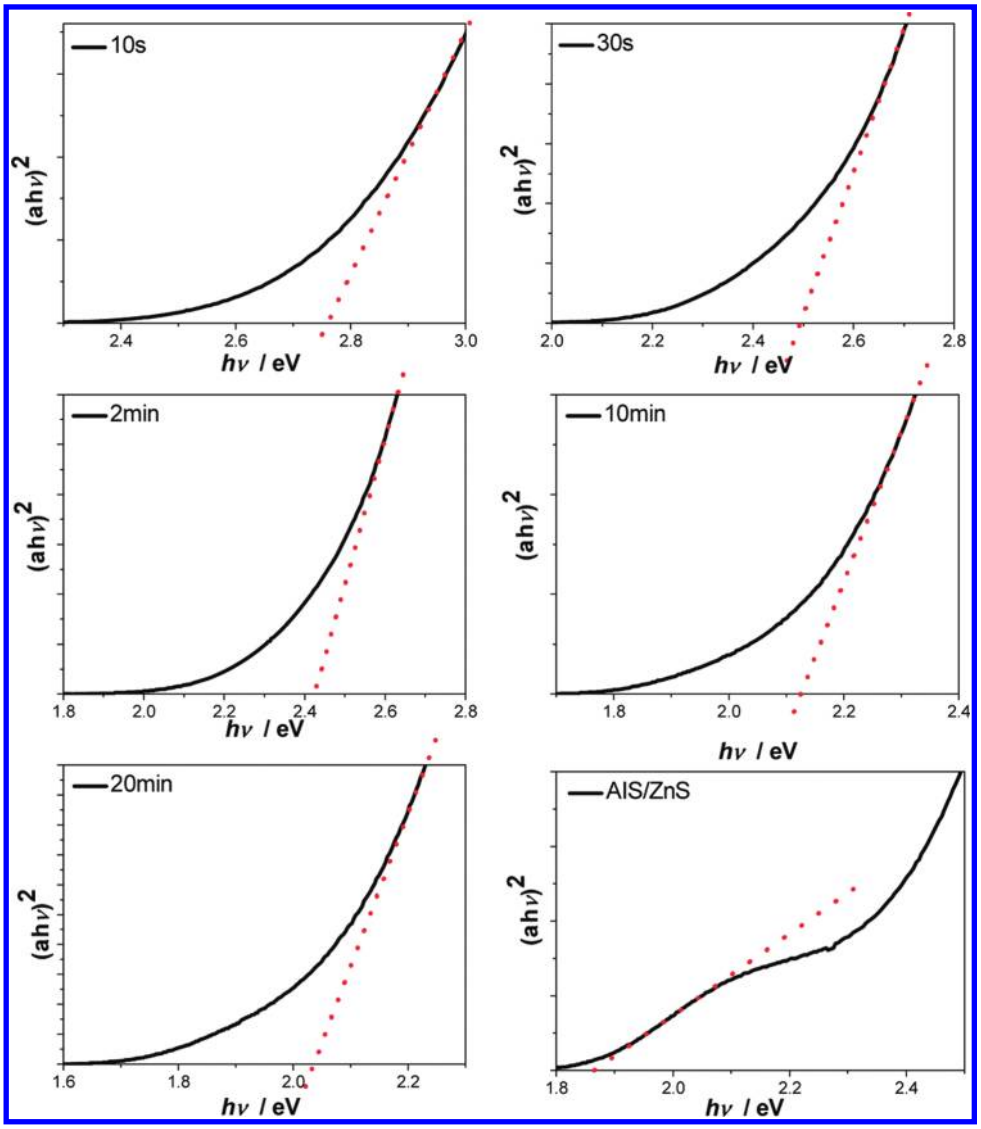

Figure 2. Estimation of the optical band gap of the AIS NCs from extrapolating the linear portion of the plot of $(\alpha h\nu)^2$ vs $h\nu$. The AIS/ZnS sample is prepared using AIS 2 min as the core coated with a ZnS shell.

Table 1. Summary of Optical Band Gaps, PL Peaks, Deconvoluted PL Peaks, and Quantum Yields (QYs) for the $AgInS_2$ NCs[a]

			deconvoluted PL peaks				
AIS	E_g	PL	Peak1	Peak2	ΔE	ratio[c]	QYs[d]
10 s[b]	449/2.76	610/2.03	605/2.05	662/1.87	57/0.18	2.05	3.0
30 s	498/2.49	625/1.98	622/1.99	677/1.83	55/0.16	1.02	3.3
2 min	512/2.42	655/1.89	625/1.99	680/1.82	55/0.17	0.27	3.1
10 min	569/2.18	702/1.77	613/2.02	710/1.75	97/0.27	0.24	2.8
20 min	596/2.08	710/1.75	620/2.00	721/1.72	101/0.28	0.23	2.8
AIS/ZnS	663/1.87	692/1.79	666/1.86	683/1.82	17/0.04	0.46	6.7

[a] The units are in nm/eV. [b] Time of NC synthesis. [c] The ratio is equal to Peak1/Peak2. [d] QYs in %.

We calculated the optical band gaps from absorption spectra by extrapolating the linear portion of the absorption slope $(\alpha h\nu)^2$ vs $h\nu$ (Figure 2).[17] Here, α is the absorption coefficient and $h\nu$ is the photon energy. This is based on the equation, $\alpha h\nu = A(h\nu - E_g)^{1/2}$, for direct-band-gap semicondutors, in which A is a constant and E_g is the optical band gap.[17] Compared with the band gap of bulk AIS at 1.87 eV,[38] our prepared AIS NCs have decreased from 2.76 to 2.08 eV with increasing the particle size. The calculated band-gap positions are tabulated in Table 1. The band gap of AIS/ZnS NCs is ~1.87 eV, lower than the corresponding AIS 2 min NCs before coating. This may be due to the decrease in surface defects and interface strain and the slightly reduced quantum confinement.

To demonstrate the size evolution with reaction time, TEM was used to characterize the NCs extracted at different durations.

dx.doi.org/10.1021/jp2011183 |J. Phys. Chem. C 2011, 115, 8945–8954

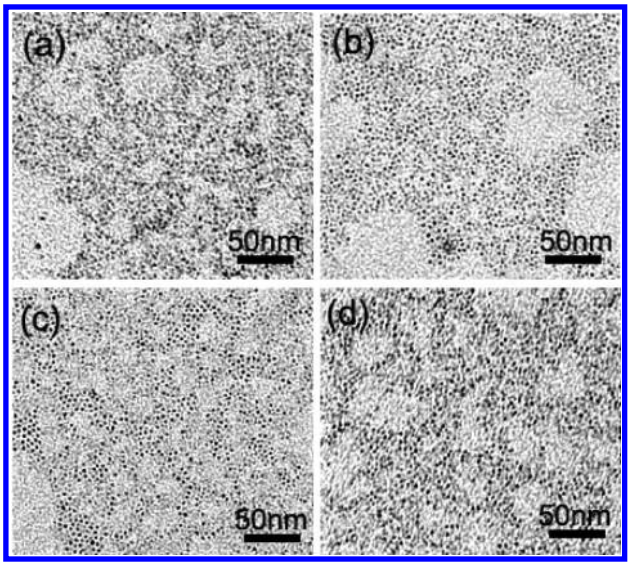

Figure 3. TEM images of the $AgInS_2$ NCs: (a) AIS 10 s, 1.9 ± 0.6 nm; (b) AIS 2 min, 2.3 ± 0.4 nm; (c) AIS 20 min, 3.1 ± 0.5 nm; and (d) AIS/ZnS (AIS 2 min coated with ZnS), 2.4 ± 0.4 nm. The corresponding size distribution of the AIS NCs is shown in Figure S1 in the Supporting Information.

The sizes of prepared AIS NCs were estimated to be 2−3 nm based on the TEM characterization, as shown in Figure 3. The sizes of the 10 s and 2 min samples are 1.9 nm (Figure 3a) and 2.3 nm (Figure 3b), respectively. With the elongation of reaction time, the NCs keep growing to larger particles with a more regular shape (~3.1 nm, Figure 3c, AIS 20 min). The ZnS-coated AIS NCs showed only a little size increase (panel b vs panel d in Figure 3), while the PL QY doubled (Table 1). The result indicates that surface defect passivation occurred during the ZnS coating.

Different from binary II−VI semiconductor QDs, the PL spectra of AIS NCs in Figure 1b have broad profiles with a typical fwhm larger than 100 nm. This is normally observed and ascribed to the donor−acceptor transition in both bulk and nanoscale ternary semiconductors.[8,18,20] The emission peaks have a maximum intensity at wavelengths ranging from 610 to 712 nm (Table 1) with QYs around 3%. Compared with previous work, these QYs are still not as high as the best results.[16,17] Similar asymmetry and large fwhms of PL were also observed in previously reported AIS[17,18] and CIS NPs.[8] We deconvoluted the PL spectra and found that each spectrum could be well fit with two Gaussian functions. Figure 4 shows the deconvolution results of the PL spectra. The peak on the spectrally blue side is referred to as Peak1, while the other one is Peak2. Besides the red shift of both peaks, the intensity ratio between the two peaks has also decreased as the size increases. We summarized PL positions, deconvoluted PL peaks, intensity ratio between PL peaks, and QYs of the PL in Table 1. In our deconvoluted spectra, the emission of Peak1 has decreased with increasing Peak2 intensity. Therefore, Peak1 and Peak2 are most likely from surface and intrinsic trap states, respectively. Another observation is that the PL shape of AIS/ZnS NCs (Figure 4f) becomes more symmetric than that of AIS 2 min (Figure 4c). After deconvolution, we found the decrease of emission at short wavelengths, which could be ascribed to the lowering in number of surface defects in high energy by ZnS coating, and when shallow surface trap states were removed, higher QYs were obtained. In the shell coating experiment, we also demonstrated that asymmetric PL peaks were not due to the coexistence of different-sized AIS NCs. Otherwise, the asymmetric shape in the PL spectra would not be eliminated by shell coating.

After steady-state UV−vis and PL measurements, TR spectroscopy was used to study trap state-related emission. Figure 5 shows the TRPL spectra of the AIS NCs at different time delays after excitation. The emission maximum of AIS 10 s (Figure 5a) has red shifted as the delay time increases (denoted by dashed lines). For AIS 2 min and 20 min NCs (Figure 5b,c), we found that the red shift is less pronounced while the ZnS-coated AIS NCs (Figure 5d) have an almost constant PL maximum. Similar red shift phenomena have been reported for CIS/ZnS I−III−VI NPs.[8] The red shifting emission indicates that PL lifetimes are wavelength-dependent, in which red emission has longer lifetimes than blue emission. As we mentioned in the steady-state PL section above, surface and intrinsic trap states contribute to the broad emission in the PL spectra of blue and red regions, respectively. Because of the high surface-to-volume ratio in nanoscale materials, surface defects, including vacancies and dangling bonds, exist in all kinds of NCs.[39−41] Surface trap states provide local sites for relaxation of photoexcited electrons, resulting in short PL lifetimes compared with deep trap states. Therefore, we found the time-resolved PL spectra red shifting due to the fast decay in the short-wavelength (higher-energy) region. In larger AIS NCs (Figure 5c), the PL emission is mainly composed of long-lived deep trap (intrinsic) states. Overall, increasing particle size suppresses surface trap states and makes the emission peak spectrally less shifting. Furthermore, we examined the TRPL spectra of ZnS-coated AIS NCs and found the nearly constant emission maximum shown in Figure 5d.

The PL decay curves in our TRPL measurements were fit by single-exponential decay functions to obtain the PL lifetimes at different emission wavelengths. Typical fitting results to derive PL lifetimes are shown in Figure 6. The same fitting procedure was performed on all AIS NCs. The fitting results as a function of wavelength are summarized in Figure 7. The PL lifetimes in the whole spectral range increase as the particle size increases. After ZnS shell coating, the lifetimes are longer than 200 ns. In our lifetime measurements of different-sized AIS NCs shown in Figure 7, the PL lifetime change along increasing wavelength depends on particle sizes and surface coating. The PL lifetime of AIS 10 s NCs keeps increasing until 700 nm in the whole spectral range. In the cases of AIS 30 s and AIS 2 min NCs, they have increased until ~650 nm and become constant between 650 and 700 nm. The large AIS NCs (AIS 10 min and 20 min) have generally constant PL lifetimes from 600 to 700 nm. After the ZnS shell coating, the results showed almost no change in PL lifetimes.

To better understand the photophysics in ternary AIS NCs, femtosecond TA spectroscopy was used to investigate the relaxation dynamics of the exciton states.[42−48] The AIS NCs were excited at the band-edge positions marked by arrows.[36,47] Figure 8 shows the TA spectra of the AIS NCs at different time intervals after excitation with steady-state absorption and emission spectra for comparison. The negative transient absorption signals ($-\Delta A$), which were red shifting as the size increases, were assigned to the lowest exciton transitions in these ternary AIS NCs. The maximum wavelength positions of these bleachings were consistent with the optical band gaps (Table 1) derived from the UV−vis absorption spectra. The bleach signals below

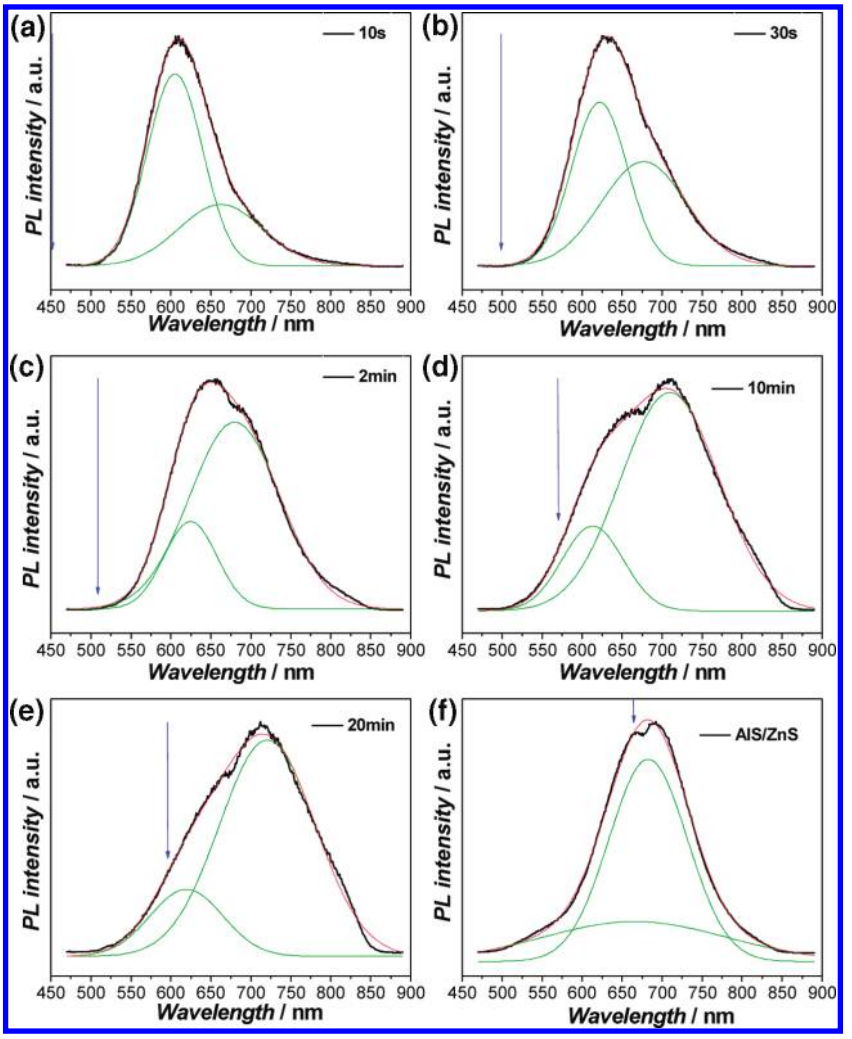

Figure 4. Gaussian deconvolution of the PL spectra of prepared $AgInS_2$ NCs. The intensity ratio (left peak/right peak) has decreased from 2.05 to 0.23 for AIS 10 s to AIS 20 min. The band-gap positions determined in Figure 2 are indicated by blue arrows. The AIS/ZnS sample is prepared using AIS 2 min as the core coated with a ZnS shell.

500 nm were not obtainable because the white light continuum was too weak in this spectral region. Figure 9 shows the summarized TA spectra (panel a) and corresponding decay kinetics (panel b) at the band-edge positions of the AIS NCs. Figure 9a shows the normalized TA spectra of AIS NCs probed at 10 ps after excitation for a better comparison of the maximum positions. Figure 9b shows the corresponding exciton dynamics with nondecay behavior within 3 ns after excitation. For our prepared AIS NCs, there is almost no bleach decay in the first 1000 ps and less than 20% decay within 3 ns. To the best of our knowledge, this is the first report on TA spectroscopy studying AIS NCs and to establish the extraordinary lifetimes of photo-induced excitons. The existence of the deep trap states in ternary AIS NCs may be responsible for these superlong-lived excitons, as discussed below.

4. DISCUSSION

Surface and intrinsic trap states play an important role here in the context of broad and asymmetric PL. We explained that two peaks in the Gaussian deconvolution (Figure 4) derive from trap state emission in terms of different transitions. Ternary I−III−VI semiconductors are known for abundant intrinsic trap states that easily form between interstitial atoms or vacancies and are responsible for donor−acceptor transitions.[20−22] Krustok et al. found that the intrinsic defects mainly include sulfur vacancies, silver vacancies, sulfur interstitials, silver interstitials, and a complex of these point defects by annealing AIS thin films in different atmospheres.[22] In addition, Hamanaka et al.[24] suggested the possible presence of silver interstitials and sulfur interstitials that act as donors and acceptors in AIS NCs, respectively, which is similar to the present work.

With the elongation of reaction time, the small NCs grow into larger particles to reduce the surface energy, the so-called Ostwald ripening, which might be the dominating process in the initial stage (AIS 10 s, 30 s, and 2 min).[49] As the NCs grow, the surface-to-volume ratio and surface tension decrease, resulting in less surface trap states. In the deconvoluted spectra, the emission of Peak1 (higher energy) decreased with simultaneously increasing Peak2 intensity. Surface trap states are usually shallow and high in energy compared with intrinsic trap states.[18,24,30] We also found a significant decrease of emission at short wavelength by ZnS coating, which could be ascribed to the reduction of surface defects at comparatively high energy. As

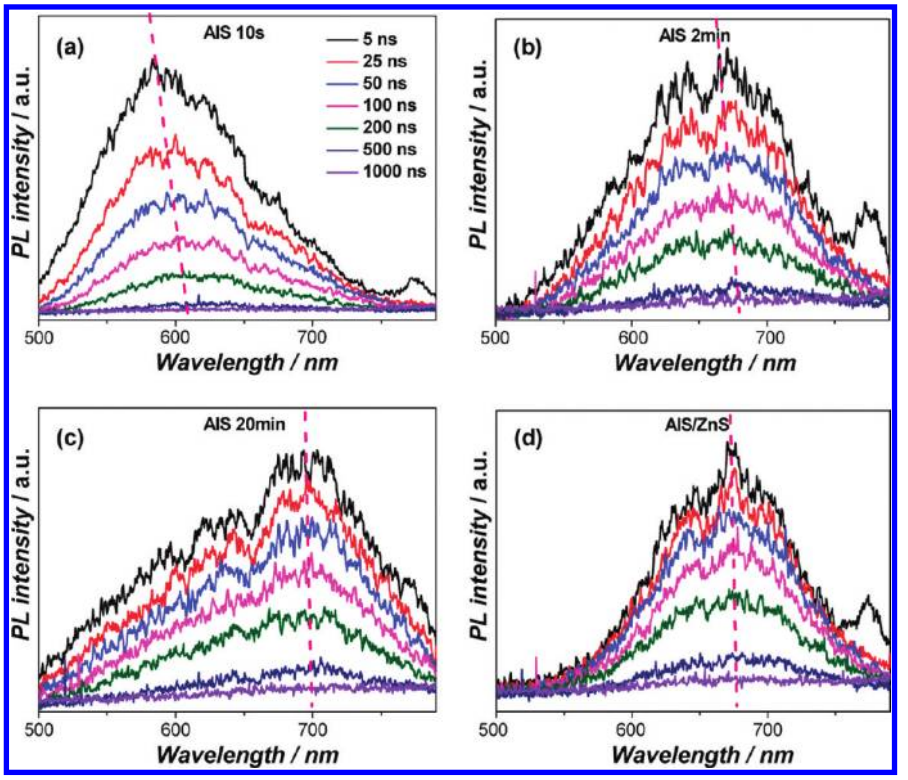

Figure 5. Time-resolved PL spectra of the AIS NCs: (a) AIS 10 s, (b) AIS 2 min, (c) AIS 20 min, and (d) AIS/ZnS. The legend in panel (a) shows the recorded time after excitation ranging from 5 to 1000 ns. Red dashed lines indicate a red shifting trend of the emission. The AIS/ZnS in (d) is made using AIS 2 min as the core coated with a ZnS shell.

shown in the TRPL spectra (Figure 5), increasing particle size suppresses surface trap states and makes the emission peak spectrally less shifting with decay time. The symmetric spectral shape in time-resolved and steady-state PL spectra both manifest the elimination of shallow trap states in AIS NCs after ZnS coating.

From the observed PL lifetime trend in Figure 7, we see that the size and coating effect determine the fraction of the surface and intrinsic trap states leading to the differences in PL responses. AIS 10 s NCs showed the most dramatic spectral shift, whereas AIS/ZnS NCs showed almost no spectral change. A similar work of PL lifetime measurements was carried out by Ogawa et al.[18] They fit the PL decay curves with biexponential decay functions and ascribed the two components to the D−A pair recombination (long-lived) and the surface defects (short-lived), respectively.[18] The PL lifetime increased dramatically (60−760 ns) along increasing wavelength in all of their NCs, quite different from our observation. They had irregular particles and a wider size distribution, which might be due to the different synthetic procedure. Both irregular shape and coexistence of different size particles make it complicated to compare the difference between Ogawa's and our work.

Recently, Li et al. reported a scalable synthesis of highly luminescent CIS NCs capped with dodecanethiol.[30] The QYs of 5−10% for CIS NCs were obtained and up to 80% for CIS/CdS NCs. In their TRPL study with a double-exponential analysis, PL decay times of 6.5 and 190 ns were measured, corresponding to the blue and red emission, respectively. Compared with the two components (6.5 and 190 ns) derived from the biexponential fitting at a fixed wavelength, we used single-exponential functions to fit the PL decays at different wavelengths (AIS and AIS/ZnS results in Figure 7). Different wavelengths are in accord with different recombination origins: surface trap states (higher energy, decay faster) and intrinsic trap states (lower energy, decay slower). Despite the different analyses between two studies, the elimination of the fast decay components in CIS/CdS and CIS/ZnS NCs is consistent with our AIS/ZnS measurements, which have a constant lifetime of ~220 ns over the entire spectral range. Both results conclude that the coating has passivated shallow surface trap states.

In the further TA spectroscopic study, there is almost no decay within 3 ns in all of our AIS NCs. TA spectra with little change within the experimental time window demonstrate clearly the extraordinary lifetimes of the photoinduced excitons. The kinetic behavior in our I−III−VI AIS NCs is quite different from that in II−VI QDs, such as CdSe and CdTe QDs, having the bleaching decay extremely fast within hundreds of picoseconds due to trapping or surface defect states.[35−37] In the context of a ternary compound study, Yumashev et al. observed a fast decay rate (~50 ps) in surface-oxidized CIS NCs.[50] They explained that the 50 ps component is due to the electron relaxation from the conduction band to midgap surface states, followed by a much long-lived decay back to the valence band. The inherently different chemical composition and reactivity between CIS and AIS NCs result in the dramatic difference of exciton lifetimes. In Li's work, both TA spectra for the CIS and CIS/CdS NCs were obtained and showed similar phenomena.[30] By changing the number of excitations per NC, they found that the band-edge bleaching was mainly due to electrons and the localized carrier must be the hole.

On the basis of the spectroscopic studies above, a summary for the identified relaxation processes in the studied AIS NCs is

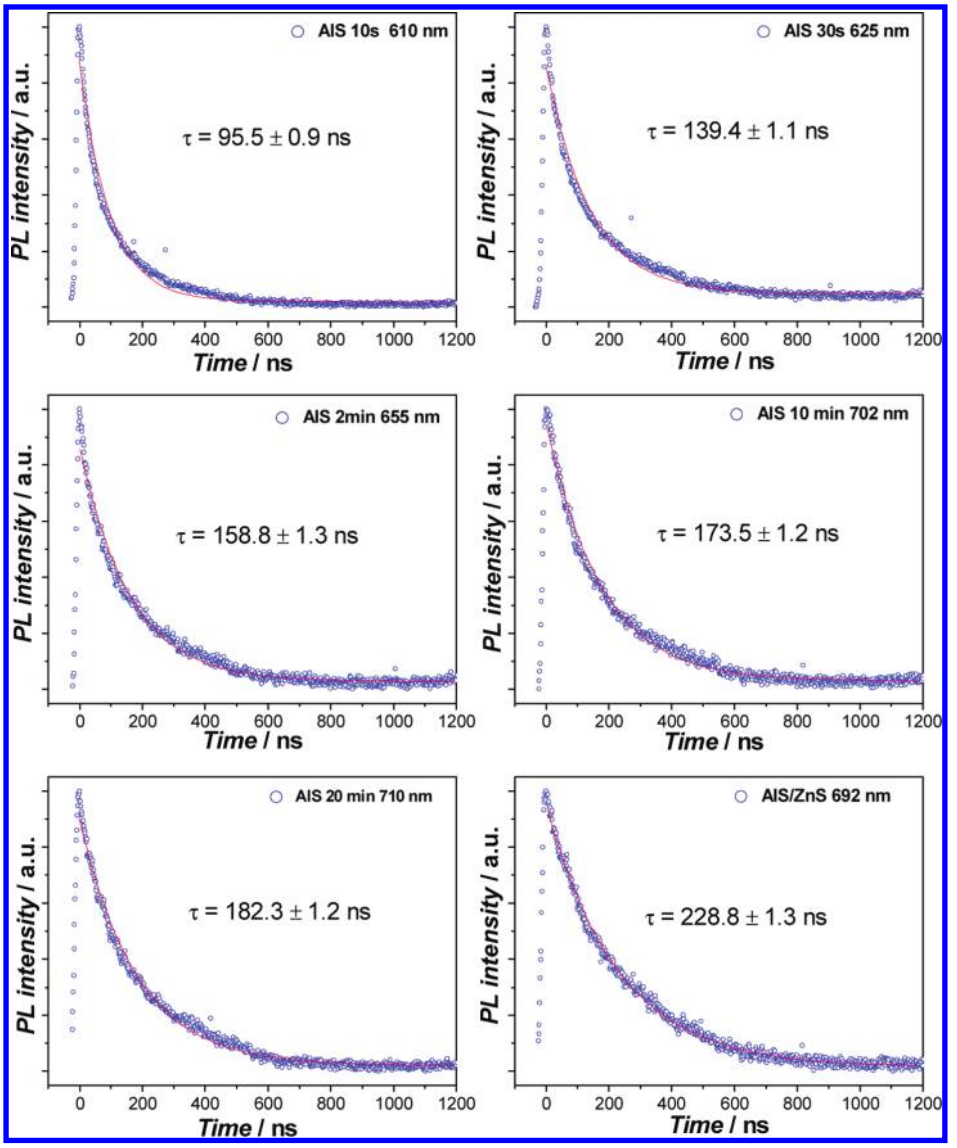

Figure 6. Acquiring PL lifetimes of the AIS NCs at the PL maximum wavelength by fitting the intensity decay curves with single-exponential functions. The PL lifetimes at different wavelengths of all AIS NCs are summarized in Figure 7.

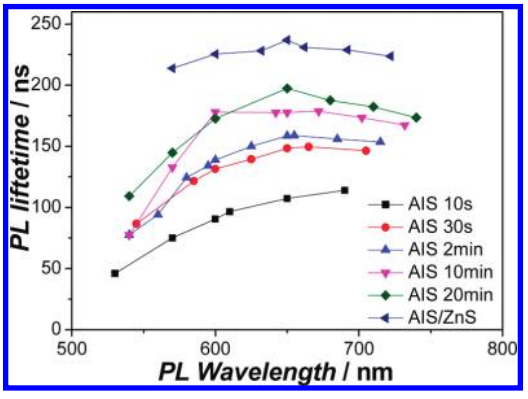

Figure 7. Wavelength-dependent PL lifetimes of the AIS NCs. All PL lifetimes at different wavelengths were obtained by single-exponential fits. The labels correspond to sample names in Table 1.

illustrated in Scheme 1. Upon photoexcitation, electrons and holes are subjected to the conduction band (CB) and the valence band (VB), respectively. In binary semiconductor NCs, electrons and holes usually combine quickly (picoseconds to nanoseconds) and give PL lifetimes of tens of nanoseconds (the dash-dotted line in Scheme 1) due to the direct band gap and surface states.[44,47,48] However, in the AIS NCs, excitons easily formed intrinsic point defects due to the existence of two kinds of differently sized cations.[18,20,22] From the TA studies, we observe that electrons stay in the CB for several nanoseconds ($\gg$3 ns in Scheme 1), followed by the relaxation to surface and intrinsic states. Surface defects, such as vacancies and dangling bonds, exist in all kinds of NCs due to the high surface-to-volume ratio in nanoscale materials. The intrinsic defects act as deep donor−acceptor pairs and are responsible for the PL in AIS NCs. In Hamanaka's work, the binding energies of the donor and acceptor were estimated to be 100 and 220 meV, respectively, from temperature-dependent time-resolved PL spectra of the 2.6 nm AIS NCs.[24] The distance between donors and acceptors (Coulomb interactions of the trapped electrons and holes) determines the transition energy, which is affected by the NC

dx.doi.org/10.1021/jp2011183 |J. Phys. Chem. C 2011, 115, 8945–8954

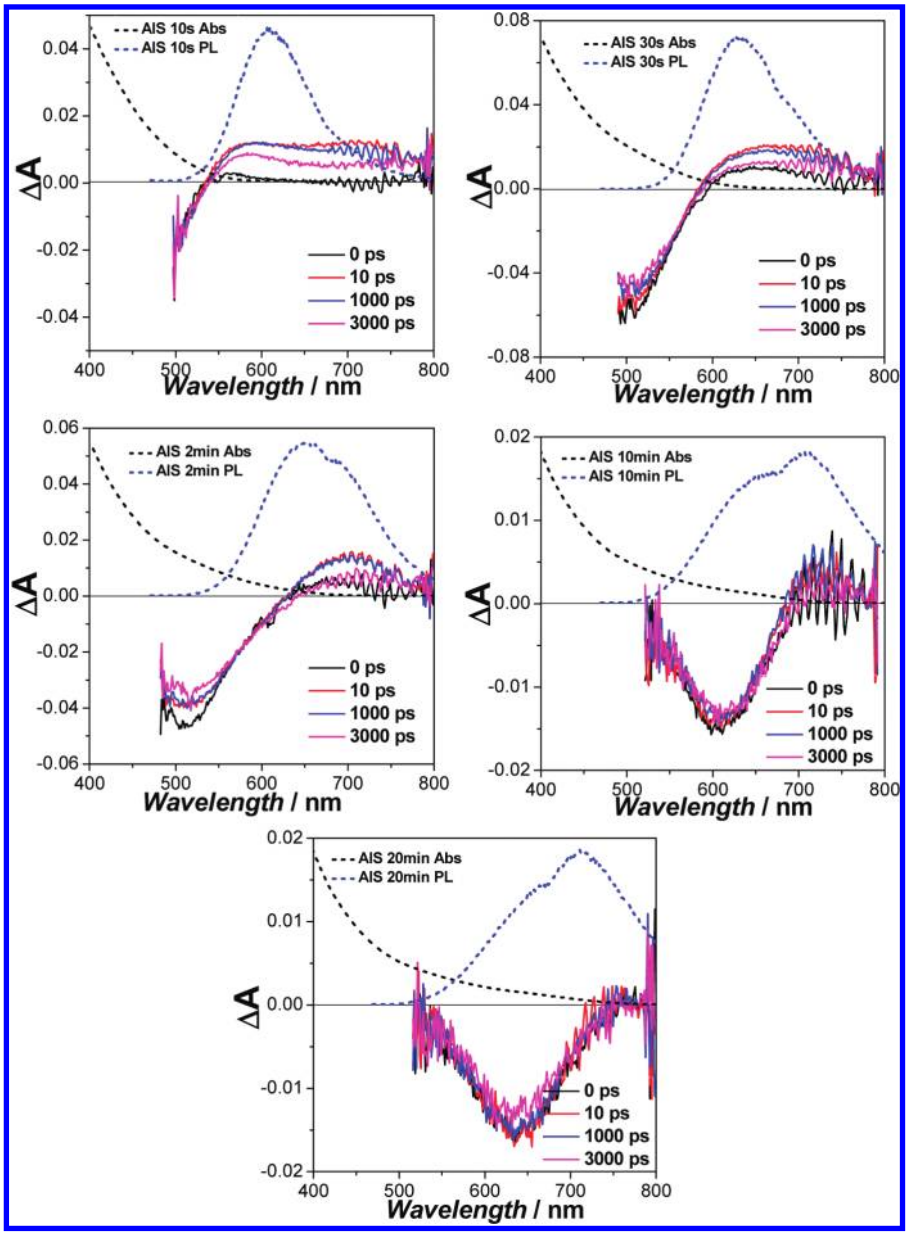

Figure 8. Transient absorption spectra of the AIS NCs. Steady-state absorption and emission spectra for the NCs (dashed lines) are added for comparison.

size, yielding high-energy emission and narrow PL band width compared with those in bulk materials.[20,24] The large fwhm and Stokes shifts were explained with the strong electron−phonon interaction of trapped carriers. The work provides a model description of the donor−acceptor transitions in AIS NCs.

We conclude that the integrated emission is dependent on intrinsic trap states, surface trap states, and band-edge recombinations, with the latest contributing the least to the overall PL in AIS ternary I−III−VI NCs. This is generally observed due to the abundance of intrinsic defects. The size of the AIS NCs determines the ratio of the radiative recombination from surface and intrinsic states, which each have distinct PL lifetimes. On the basis of the TRPL studies, the surface and intrinsic states have lifetimes of ∼50 and ∼220 ns, respectively (shown in Scheme 1). The long-lived excitons and broad band absorption of the prepared AIS NCs may provide potential applications in the design of photocatalysts and photovoltaics.

5. CONCLUSIONS

In this work, we presented the preparation of $AgInS_2$ NCs with tunable sizes synthesized at low temperature. Steady-state UV−vis absorption and PL spectroscopies were used to characterize the absorption and emission properties of the prepared AIS NCs. As the particle size increased, we observed a red shift in both absorption and PL spectra due to the reduced quantum confinement. The asymmetric shape of the PL bands was fit with two Gaussian functions, which were assigned to surface and intrinsic trap states, respectively. The size increase and shell coating were found to eliminate surface trap states. Time-resolved PL spectroscopy was used to investigate wavelength- and size-dependent PL lifetimes in the prepared AIS and AIS/ZnS NCs. The red shifting PL with increasing decay times indicates that the PL originates from trap states of different energies. Easily formed intrinsic point defects act as deep

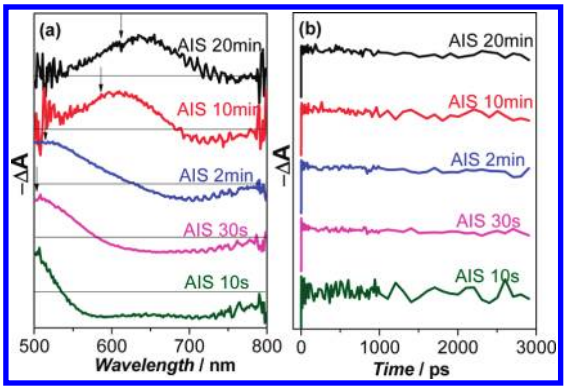

Figure 9. (a) Transient absorption spectra of AIS NCs recorded at 10 ps after excitation. The arrows indicate the pumping positions near the band gaps, as tabulated in Table 1. (b) Corresponding kinetics at the band-edge positions of the AIS NCs. The bleach signals stay constant in a 3 ns time window after excitation, highlighting the long-lived excitons in the AIS NCs.

Scheme 1. Schematic of the Relaxation Dynamics in the Investigated $AgInS_2$ Nanocrystals

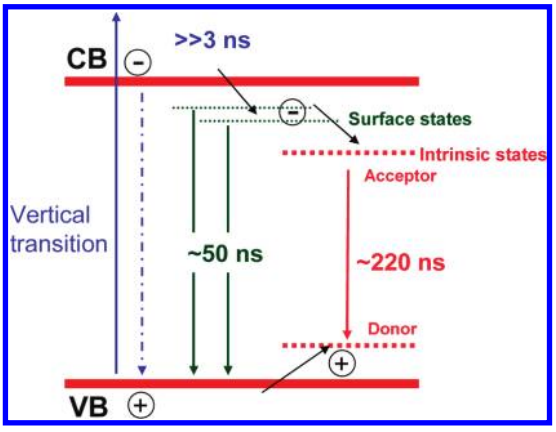

donor−acceptor pairs that dominate the optical properties of the ternary AIS NCs. This work reports the first femtosecond time-resolved transient absorption spectroscopy measurements to study the population dynamics of exciton states in ternary AIS NCs. An extremely long-lived excitation (≫3 ns, which was the experimental time window) was observed for all of the studied AIS NCs. The long-lived exciton and broad visible absorption could potentially furnish materials for optoelectronic applications, such as photocatalysis and photovoltaics.

■ ASSOCIATED CONTENT

Supporting Information. Size distribution of the AIS NCs. This material is available free of charge via the Internet at http://pubs.acs.org.

■ AUTHOR INFORMATION

Corresponding Author

*E-mail: burda@case.edu. Phone: (216) 368-5918. Fax: (216) 368-3006.

■ ACKNOWLEDGMENT

C.B. is grateful for support from the NSF (Career CHE-0239688) and NIRT (CTS-0608896).

■ REFERENCES

(1) Shay, J. L.; Wernick, J. H. Ternary Chalcopyrite Semiconductors: Growth, Electronic Properties, And Applications; Pergamon Press: Oxford, U.K., 1975.
(2) Klenk, R.; Klaer, J.; Scheer, R.; Lux-Steiner, M. C.; Luck, I.; Meyer, N.; Ruhle, U. *Thin Solid Films* **2005**, *480*, 509.
(3) Tsuji, I.; Kato, H.; Kudo, A. *Angew. Chem., Int. Ed.* **2005**, *44*, 3565.
(4) Allen, P. M.; Bawendi, M. G. *J. Am. Chem. Soc.* **2008**, *130*, 9240.
(5) Omata, T.; Nose, K.; Otsuka-Yao-Matsuo, S. *J. Appl. Phys.* **2009**, *105*, 073106.
(6) Li, L.; Coates, N.; Moses, D. *J. Am. Chem. Soc.* **2010**, *132*, 22.
(7) Panthani, M. G.; Akhavan, V.; Goodfellow, B.; Schmidtke, J. P.; Dunn, L.; Dodabalapur, A.; Barbara, P. F.; Korgel, B. A. *J. Am. Chem. Soc.* **2008**, *130*, 16770.
(8) Li, L.; Daou, T. J.; Texier, I.; Tran, T. K. C.; Nguyen, Q. L.; Reiss, P. *Chem. Mater.* **2009**, *21*, 2422.
(9) Pons, T.; Pic, E.; Lequeux, N.; Cassette, E.; Bezdetnaya, L.; Guillemin, F.; Marchal, F.; Dubertret, B. *ACS Nano* **2010**, *4*, 2531.
(10) Yong, K. T.; Roy, I.; Hu, R.; Ding, H.; Cai, H. X.; Zhu, J.; Zhang, X. H.; Bergey, E. J.; Prasad, P. N. *Integr. Biol.* **2010**, *2*, 121.
(11) Wang, L. L.; Zheng, H. Z.; Long, Y. J.; Gao, M.; Hao, J. Y.; Du, J.; Mao, X. J.; Zhou, D. B. *J. Hazard. Mater.* **2010**, *177*, 1134.
(12) Du, W. M.; Qian, X. F.; Yin, J.; Gong, Q. *Chem.—Eur. J.* **2007**, *13*, 8840.
(13) Tian, L.; Vittal, J. J. *New J. Chem.* **2007**, *31*, 2083.
(14) Torimoto, T.; Adachi, T.; Okazaki, K.; Sakuraoka, M.; Shibayama, T.; Ohtani, B.; Kudo, A.; Kuwabata, S. *J. Am. Chem. Soc.* **2007**, *129*, 12388.
(15) Wang, D. S.; Zheng, W.; Hao, C. H.; Peng, Q.; Li, Y. D. *Chem. Commun.* **2008**, 2556.
(16) Xie, R. G.; Rutherford, M.; Peng, X. G. *J. Am. Chem. Soc.* **2009**, *131*, 5691.
(17) Feng, Z. Y.; Dai, P. C.; Ma, X. C.; Zhan, J. H.; Lin, Z. J. *Appl. Phys. Lett.* **2010**, *96*, 013104.
(18) Ogawa, T.; Kuzuya, T.; Hamanaka, Y.; Sumiyama, K. *J. Mater. Chem.* **2010**, *20*, 2226.
(19) Okamoto, K.; Kinoshita, K. *Solid-State Electron.* **1976**, *19*, 31.
(20) Redjai, E.; Masse, G. *Phys. Status Solidi B* **1985**, *131*, K157.
(21) Masse, G.; Redjai, E. *J. Appl. Phys.* **1986**, *59*, 1544.
(22) Krustok, J.; Raudoja, J.; Krunks, M.; Mandar, H.; Collan, H. *J. Appl. Phys.* **2000**, *88*, 205.
(23) You, S. H.; Hong, K. J.; Youn, C. J.; Jeong, T. S.; Moon, J. D.; Kim, H. S.; Park, J. S. *J. Appl. Phys.* **2001**, *90*, 3894.
(24) Hamanaka, Y.; Ogawa, T.; Tsuzuki, M.; Kuzuya, T. *J. Phys. Chem. C* **2011**, *115*, 1786.
(25) Kameyama, T.; Okazaki, K. I.; Ichikawa, Y.; Kudo, A.; Kuwabata, S.; Torimoto, T. *Chem. Lett.* **2008**, *37*, 700.
(26) Uematsu, T.; Taniguchi, S.; Torimoto, T.; Kuwabata, S. *Chem. Commun.* **2009**, 7485.
(27) Torimoto, T.; Ogawa, S.; Adachi, T.; Kameyama, T.; Okazaki, K. I.; Shibayama, T.; Kudo, A.; Kuwabata, S. *Chem. Commun.* **2010**, *46*, 2082.
(28) Nose, K.; Fujita, N.; Omata, T.; Otsuka-Yao-Matsuo, S. *J. Phys.: Conf. Ser.* **2009**, *165*, 012028.
(29) Zhong, H.; Lo, S. S.; Mirkovic, T.; Li, Y.; Ding, Y.; Li, Y.; Scholes, G. D. *ACS Nano* **2010**, *4*, 5253.
(30) Li, L.; Pandey, A.; Werder, D. J.; Khanal, B. P.; Pietryga, J. M.; Klimov, V. I. *J. Am. Chem. Soc.* **2011**, *133*, 1176.
(31) Zhong, H. Z.; Zhou, Y.; Ye, M. F.; He, Y. J.; Ye, J. P.; He, C.; Yang, C. H.; Li, Y. F. *Chem. Mater.* **2008**, *20*, 6434.
(32) Gaigalas, A. K.; Wang, L. L. *J. Res. Natl. Inst. Stand. Technol.* **2008**, *113*, 17.

(33) Lou, Y. B.; Samia, A. C. S.; Cowen, J.; Banger, K.; Chen, X. B.; Lee, H.; Burda, C. *Phys. Chem. Chem. Phys.* **2003**, *5*, 1091.
(34) Lou, Y. B.; Chen, X. B.; Samia, A. C.; Burda, C. *J. Phys. Chem. B* **2003**, *107*, 12431.
(35) Dayal, S.; Burda, C. *J. Am. Chem. Soc.* **2007**, *129*, 7977.
(36) Chuang, C. H.; Lo, S. S.; Scholes, G. D.; Burda, C. *J. Phys. Chem. Lett.* **2010**, *1*, 2530.
(37) Dayal, S.; Krolicki, R.; Lou, Y.; Qiu, X.; Berlin, J. C.; Kenney, M. E.; Burda, C. *Appl. Phys. B* **2006**, *84*, 309.
(38) Shay, J. L.; Tell, B.; Schiavon, L. M.; Kasper, H. M.; Thiel, F. *Phys. Rev. B* **1974**, *9*, 1719.
(39) Burda, C.; Chen, X. B.; Narayanan, R.; El-Sayed, M. A. *Chem. Rev.* **2005**, *105*, 1025.
(40) Guyot-Sionnest, P.; Hines, M. A. *Appl. Phys. Lett.* **1998**, *72*, 686.
(41) Guyot-Sionnest, P.; Shim, M.; Matranga, C.; Hines, M. *Phys. Rev. B* **1999**, *60*, R2181.
(42) Burda, C.; Link, S.; Mohamed, M. B.; El-Sayed, M. *J. Chem. Phys.* **2002**, *116*, 3828.
(43) Braun, M.; Burda, C.; Mohamed, M.; El-Sayed, M. *Phys. Rev. B* **2001**, *6403*, 035317.
(44) Klimov, V. I. *J. Phys. Chem. B* **2000**, *104*, 6112.
(45) Burda, C.; El-Sayed, M. A. *Pure Appl. Chem.* **2000**, *72*, 165.
(46) Burda, C.; Link, S.; Green, T. C.; El-Sayed, M. A. *J. Phys. Chem. B* **1999**, *103*, 10775.
(47) Kambhampati, P. *Acc. Chem. Res.* **2011**, *44*, 1.
(48) Huxter, V. M.; Scholes, G. D. J. *Nanophotonics* **2009**, *3*, 16.
(49) Norako, M. E.; Franzman, M. A.; Brutchey, R. L. *Chem. Mater.* **2009**, *21*, 4299.
(50) Yumashev, K. V.; Malyarevich, A. M.; Prokoshin, P. V.; Posnov, N. N.; Mikhailov, V. P.; Gurin, V. S.; Artemyev, M. V. *Appl. Phys. B* **1997**, *65*, 545.